amcs

2–D LOSSLESS FIR FILTER DESIGN USING SYNTHESIS OF THE PARAUNITARY TRANSFER FUNCTION MATRIX

KRZYSZTOF WAWRYN [a], PAWEŁ POCZEKAJŁO [a,*]

[a] Department of Digital Signal Processing Systems
Koszalin University of Technology
ul. Śniadeckich 2, 75-453 Koszalin, Poland
e-mail: `pawel.poczekajlo@tu.koszalin.pl`

A synthesis method for designing two-dimensional lossless finite impulse response (FIR) filters for various digital signal processing tasks is proposed. The synthesis method is based on using a 2-D embedding approach to obtain the paraunitary transfer function matrix of the lossless FIR filter. The elements of the paraunitary transfer function matrix are the transfer function of a given lossy FIR structure and the transfer functions for its complementary structures. The embedding method is used to design complementary FIR filter structures for several known lossy FIR filters. The lossless FIR filter matrix obtained in this article has a size of 3×1 and satisfies the paraunitary conditions. The conditions are described by a set of nonlinear equations. A modified Newton method is used to solve this set of equations. The proposed design method is used to determine the lossless structures of two-dimensional FIR filters for various digital processing tasks.

Keywords: lossless system, paraunitary transfer function matrix, FIR filter, embedding method.

1. Introduction

Lossless filters preserve energy and have good properties such as stability, a low sensitivity to changes in their parameters, and no parasitic oscillations (Belevitch, 1968; Fettweis, 1971; Deprettere and Dewilde, 1980; Rao and Dewilde, 1987; Fettweis, 1991). In recent years, lossless FIR filters have become very attractive among scientists and designers, because these filters have various research and engineering applications (Vaidyanathan and Mitra, 2019; Wang *et al.*, 2020; Valkova-Jarvis *et al.*, 2019). For example, the lossless structures of filter banks are very popular in practical applications (Yang *et al.*, 2017; Stancic *et al.*, 2018; Liu *et al.*, 2017). FIR filters are widely used in image processing, e.g., in edge detection and the blurring or sharpening of an image. They are usually lossy filters. The corresponding lossless FIR filters can be obtained using orthogonal transformations (Fettweis, 1982; Soman and Vaidyanathan, 1995; Wawryn and Wirski, 2009; Dewilde, 2019).

Lossless filters are orthogonal filters and are usually described by an orthogonal state space matrix or, equivalently, by a paraunitary transfer function matrix.

The search for a one-dimensional (1-D) lossless 2-port FIR filter is based on the synthesis of a transfer function matrix that would have the required properties, such as a given frequency response. This method is called embedding, and it can be defined as follows: for a given 1-D scalar transfer function $H(z)$, a paraunitary transfer function matrix $\mathbf{H}(z)$, such that one of its elements is equal to $H(z)$, should be found, and

$$\mathbf{H}^{\mathrm{T}}(z^{-1})\mathbf{H}(z) = \mathbf{I}. \tag{1}$$

Synthesis methods for a paraunitary transfer function matrix of higher-dimension filters were described by Fettweis (1991), the properties of the 2×2 paraunitary transfer function matrix were studied by Fettweis (1982), and the method of factorization for such matrices was presented by Basu and Fettweis (1985). The synthesis of n-D systems is difficult because it requires a set of n nonlinear equations to be solved in order to find an embedding for a given n-D transfer function. Bose and Strintzis (1973) presented a method based on the factorisation of the n-D matrix, but it does not provide a 100% guarantee of finding a solution. It uses Hilbert's solution to the problem of whether a non-negative real form of even degree m in n variables is always a sum

of squares (SOS) of other real forms. A similar method was used by Piekarski and Wirski (2005) to obtain a two-dimensional (2-D) embedding. Lossless systems with a paraunitary transfer function matrix can also be obtained using the Roesser model (Roesser, 1975; Wirski and Wawryn, 2008; Kaczorek, 2008; Kaczorek and Rogowski, 2010).

The typical size of the paraunitary transfer function matrix is 2×2. A square matrix ($n \times n$) is used when the filter should possess equal numbers of inputs and outputs. It is often implemented using state space equations. However, the paraunitary transfer function matrix need not always be square. An example of such an approach is presented by Wirski (2008). A non-square matrix is also applied in the method presented in this article.

There are plenty of existing FIR filters. In the vast majority of cases, they are lossy filters and suffer from instability, a lack of robustness on rounding, a high sensitivity to changes in the filter parameters, etc. To overcome these obstacles, the main aim of this article is to design a lossless system by combining a given FIR filter structure and its complementary structures to create a structure with the lossless property. In this case, the given filter is able to use the advantages of the whole system (lossless system). Such a lossless system is described by the paraunitary transfer function matrix. The elements of the paraunitary transfer function matrix are the transfer functions of the given FIR filter structure and its complementary structures. The transfer function of the given filter structure is known, while the transfer functions of the complementary structures have to be found. The transfer functions of complementary structures are found using embedding. The proposed lossless FIR filter design method is based on the synthesis of a paraunitary transfer function matrix that describes the lossless filter together with its given and complementary structures. This synthesis using embedding leads to a set of nonlinear equations, which are solved using Newton's method.

The paraunitary transfer function matrix condition (1) and the conditions for the 2-D and higher-order cases are expressed as a set of very-high-order polynomials. Therefore, as for most non-linear sets of equations, it is very difficult to guarantee the convergence of the method used to find the local solution and nearly impossible to find a global solution. In this article, the size of the paraunitary 2-D transfer function matrix is 3×1 and a modified Newton's method (Golub and Loan, 1996) is used to find the solution of the paraunitary condition.

The article is organized as follows. In Section 2, the paraunitary transfer function matrix condition of the 2-D lossless FIR filters and the impulse responses of linear FIR filters with quadrantal and octagonal symmetry are formulated. The synthesis of the 2-D paraunitary

transfer function matrix, which leads to a set of non-linear equations, is presented in Section 3. Solving a system of nonlinear equations using the modified Newton's method is described in Section 4. Several different practical examples of using 2-D FIR filters to search for their lossless counterparts are presented in Section 5. Finally, conclusions are drawn in Section 6.

2. 2-D lossless FIR filters: Problem formulation

In this paper, an original embedding method to search for 2-D lossless FIR filters is presented. The method makes it possible to determine paraunitary transfer function matrices, enabling the implementation of many lossy transfer functions that are used in practice.

The FIR transfer function $H(z_1, z_2)$ for which the embedding procedure is carried out must be a stable rational (Fettweis, 1991), which means that the following conditions are satisfied:

all poles are in ($|z_1| < 1$ and $|z_2| < 1$) and
$$\forall_{w_1, w_2} (|H(e^{jw_1}, e^{jw_2}|^2) \leq 1. \quad (2)$$

To satisfy the conditions (2), for the primary $\widehat{H}(z_1, z_2)$, the scaling factor H_{MAX} must be applied:

$$H(z_1, z_2) = \frac{\widehat{H}(z_1, z_2)}{H_{\text{MAX}}}, \quad (3)$$

where H_{MAX} is the maximum value of an amplitude characteristic of $\widehat{H}(z_1, z_2)$.

The embedding resulting in the paraunitary matrix is defined as follows. For a given 2-D transfer function $H(z_1, z_2)$, a paraunitary transfer function matrix $\mathbf{H}(z_1, z_2)$ has to satisfy the following requirements: one of its elements equals $H(z_1, z_2)$ and

$$\mathbf{H}^{\text{T}}(z_1^{-1}, z_2^{-1})\mathbf{H}(z_1, z_2) = \mathbf{I}. \quad (4)$$

The transfer function of the 2-D FIR filter can be expressed as follows:

$$H(z_1, z_2) = \sum_{i=0}^{N_1-1} \sum_{j=0}^{N_2-1} h_{ij} z_1^{-i} z_2^{-j} = \mathbf{z}_1^{\text{T}} \mathbf{H} \mathbf{z}_2, \quad (5)$$

where N_1 and N_2 are positive integers, $\mathbf{H} \in \mathbb{R}^{N_1 \times N_2}$,

$$\mathbf{z}_1 = \left[1 \; z_1^{-1} \ldots z_1^{-(N_1-1)} \right]^{\text{T}},$$

$$\mathbf{z}_2 = \left[1 \; z_2^{-1} \ldots z_2^{-(N_2-1)} \right]^{\text{T}}.$$

In practical applications, non-linear or linear 2-D FIR filters are characterized by an impulse response, and those

with a linear phase response and odd values of N_1 and N_2 are mainly used.

For odd values of N_1 and N_2, a 2-D FIR filter response with a linear phase and constant group delay can be obtained throughout the entire baseband. The impulse response of the filter is symmetrical around the shifted origin O'(n_1, n_2) (Lu and Antoniou, 1992; Charalambous, 1985), where

$$n_i = \frac{N_i - 1}{2}, \tag{6}$$

for $i = 1, 2$, and the following conditions must hold:

$$h_{ij} = h_{N_1-1-i \ N_2-1-j}, \tag{7}$$

for $0 \le i \le N_1 - 1, 0 \le j \le N_2 - 1$.

If quadrantal symmetry in the 2-D linear phase is desired and a constant-group-delay FIR filter is also required, then the following conditions (Charalambous, 1985) must hold:

$$h_{ij} = h_{i \ N_2-1-j} = h_{N_1-1-i \ j}, \tag{8}$$

for $0 \le i \le \frac{N_1-1}{2}, 0 \le j \le \frac{N_2-1}{2}$.

If octagonal symmetry in the 2-D linear phase is desired and a constant-group-delay FIR filter is also required, then additional conditions (Charalambous, 1985) must hold:

$$N_1 = N_2 = N, \tag{9}$$

$$h_{ij} = h_{ji}, \tag{10}$$

for $0 \le i \le \frac{N-1}{2}, 0 \le j \le \frac{N-1}{2}$.

In some applications, only a group delay is required. Then, for odd values of N_1 and N_2, the impulse response is antisymmetric around the shifted origin O'(n_1, n_2) (6), and the following conditions (Lu and Antoniou, 1992) must hold:

$$h_{ij} = -h_{N_1-1-i \ N_2-1-j}, \tag{11}$$

for $0 \le i \le \frac{N_1-1}{2}, 0 \le j \le \frac{N_2-1}{2}$.

3. Synthesis of the 2-D paraunitary transfer function matrix

In order to obtain an embedding for the lossy $H(z_1, z_2)$ resulting in the paraunitary $\mathbf{H}(z_1, z_2)$, it is necessary to introduce N_p additional transfer functions of the form

$$G_p(z_1, z_2) = \sum_{i=0}^{N_1-1} \sum_{j=0}^{N_2-1} g_{pij} z_1^{-i} z_2^{-j} = \mathbf{z}_1^{\mathrm{T}} \mathbf{G}_p \mathbf{z}_2, \tag{12}$$

for $p = 1, 2, \ldots, N_p$, where N_1 and N_2 are odd integers,

$$\mathbf{z}_1 = \left[1 \ z_1^{-1} \ \ldots \ z_1^{-(N_1-1)} \right]^{\mathrm{T}},$$

$$\mathbf{z}_2 = \left[1 \ z_2^{-1} \ \ldots \ z_2^{-(N_2-1)} \right]^{\mathrm{T}},$$

$\mathbf{G}_p \in \mathbb{R}^{N_1 \times N_2}$, and the proposed embedding is expressed as follows:

$$\mathbf{H}(z_1, z_2) = \begin{bmatrix} H(z_1, z_2) \\ G_1(z_1, z_2) \\ \vdots \\ G_{N_p}(z_1, z_2) \end{bmatrix}. \tag{13}$$

N_p should be a minimal number for which the paraunitary condition (4) is satisfied. Taking into account (13), the paraunitary condition (4) is expressed as follows:

$$\mathbf{H}^{\mathrm{T}} \left(z_1^{-1}, z_2^{-1} \right) \mathbf{H} \left(z_1, z_2 \right) = 1. \tag{14}$$

The FIR filter described by the paraunitary condition (14) is a stable all-pass filter and the following power complementary property holds (Fettweis, 1991; Vaidyanathan and Mitra, 2019; Smith III, 2007):

$$\left| H \left(e^{j\omega_1}, e^{j\omega_2} \right) \right|^2 + \sum_{p=1}^{N_p} \left| G_p \left(e^{j\omega_1}, e^{j\omega_2} \right) \right|^2 = 1. \tag{15}$$

Equation (14) can be expressed as follows:

$$\begin{aligned} \mathbf{H}^{\mathrm{T}} &\left(z_1^{-1}, z_2^{-1} \right) \mathbf{H} \left(z_1, z_2 \right) \\ &= H \left(z_1^{-1}, z_2^{-1} \right) H \left(z_1, z_2 \right) \\ &\quad + \sum_{p=1}^{N_p} G_p \left(z_1^{-1}, z_2^{-1} \right) G_p \left(z_1, z_2 \right) = 1. \end{aligned} \tag{16}$$

Equation (14) can be also rearranged into the form of

$$\begin{aligned} \mathbf{H}^{\mathrm{T}} &\left(z_1^{-1}, z_2^{-1} \right) \mathbf{H} \left(z_1, z_2 \right) \\ &= \sum_{k=-N_1+1}^{N_1-1} \sum_{l=-N_2+1}^{N_2-1} C_{kl} z_1^k z_2^l = 1. \end{aligned} \tag{17}$$

Equation (17) is satisfied when $C_{00} = 1$ and $C_{kl} = 0$ for all $k = -N_1+1, \ldots, N_1-1, l = -N_2+1, \ldots, N_2-1$, $k = l \ne 0$, and the total number of coefficients equals $(2N_1 - 1)(2N_2 - 1)$.

Due to the symmetry of the coefficients in (17) around the origin O'$(0, 0)$, the following relations hold:

$$C_{kl} = C_{-k \ -l}, \tag{18}$$

for all $k = -N_1+1, \ldots, N_1-1, l = -N_2+1, \ldots, N_2-1$, and $k = l \ne 0$.

Due to the same coefficients h_{ij} being in the transfer functions $H(z_1^{-1}, z_2^{-1})$ and $H(z_1, z_2)$, and due to the same relations of the coefficients being in the transfer functions $G_1, G_2, \ldots, G_{N_p}$, the coefficients C_{kl} and $C_{-k,-l}$ in the products $C_{kl} z_1^k z_2^l$ and $C_{-k-l} z_1^{-k} z_2^{-l}$ in (17) are the same. Then, according to this symmetry, half of the coefficients of $(2N_1 - 1)(2N_2 - 1) - 1$ have identical

counterparts. Only the coefficient C_{00} has no equivalent. This means that the number of determined coefficients is

$$m = \frac{(2N_1 - 1)(2N_2 - 1) - 1}{2} + 1. \qquad (19)$$

After some algebra, (19) can be expressed as

$$m = N_1 N_2 + (N_1 - 1)(N_2 - 1). \qquad (20)$$

By substituting (5) and (12) into (16), substituting (18) into (17), and comparing the coefficients in (16) and (17), the m calculated coefficients (20) can be expressed as follows:

$$C_{kl} = \sum_{j=l}^{N_2-1} \sum_{i=k}^{N_1-1} (h_{ij}\, h_{i-k\; j-l}$$
$$+ \sum_{p=1}^{N_p} g_{pij}\, g_{p\; i-k\; j-l}) = 1$$
$$\text{for } k = l = 0,$$

$$C_{kl} = \sum_{j=l}^{N_2-1} \sum_{i=k}^{N_1-1} (h_{ij}\, h_{i-k\; j-l}$$
$$+ \sum_{p=1}^{N_p} g_{pij}\, g_{p\; i-k\; j-l}) = 0 \qquad (21)$$
$$\text{for } k = 0, 1, \ldots, N_1 - 1,$$
$$l = 0, 1, \ldots, N_2 - 1,$$
$$\text{and } k = l \neq 0,$$

$$C_{kl} = \sum_{j=l}^{N_2-1} \sum_{i=0}^{N_1-1+k} (h_{ij}\, h_{i-k\; j-l}$$
$$+ \sum_{p=1}^{N_p} g_{pij}\, g_{p\; i-k\; j-l}) = 0$$
$$\text{for } k = -N_1 + 1, \ldots, -2, -1$$
$$\text{and } l = 1, 2, \ldots, N_2 - 1.$$

The set of equations (21) describes a system composed of $m = N_1 N_2 + (N_1 - 1)(N_2 - 1)$ non-linear equations with $n = N_p N_1 N_2$ independent variables g_{pij}. The locations of m coefficients calculated using (21) are depicted in Fig. 1.

The equations for $C_{N_1-1\; N_2-1}$ and $C_{-N_1+1\; N_2-1}$ in (21) are expressed as follows:

$$C_{N_1-1\; N_2-1} = h_{N_1-1\; N_2-1}\, h_{00}$$
$$+ \sum_{p=1}^{N_p} g_{p\; N_1-1\; N_2-1}\, g_{p00} = 0,$$
$$C_{-N_1+1\; N_2-1} = h_{0\; N_2-1}\, h_{N_1-1\; 0} \qquad (22)$$
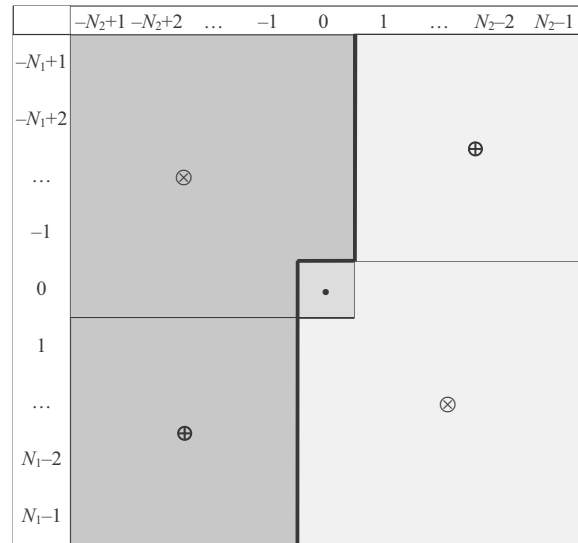$$+ \sum_{p=1}^{N_p} g_{p\; 0\; N_2-1}\, g_{p\; N_1-1\; 0} = 0.$$

Fig. 1. Locations of m coefficients calculated using (21) are depicted in bright grey and medium grey (coefficient C_{00}). Due to the symmetry in (18), the coefficients depicted in dark grey are not calculated.

If the matrix $\mathbf{H}$ describes a system with a linear phase, then according to the symmetry described by (8), h_{00} equals $h_{N_1-1\; N_2-1}$ and $h_{0\; N_2-1}$ equals $h_{N_1-1\; 0}$. Consequently, the equations (22) can be rearranged into the following form:

$$C_{N_1-1\; N_2-1}$$
$$= h_{00}^2 + \sum_{p=1}^{N_p} g_{p\; N_1-1\; N_2-1}\, g_{p00} = 0,$$
$$C_{-N_1+1, N_2-1} \qquad (23)$$
$$= h_{0\; N_2-1}^2 + \sum_{p=1}^{N_p} g_{p\; 0\; N_2-1}\, g_{p\; N_1-1\; 0} = 0.$$

For non-zero h_{00} and $h_{0\; N_1-1}$, at least one of the transfer functions $G_p(z_1, z_2)$ for $p = 1, 2, \ldots, N_p$ must describe a system with a non-linear phase, where $g_{p\; N_1-1\; N_2-1} \neq g_{p00}$ and $g_{p\; 0\; N_2-1} \neq g_{p\; N_1-1\; 0}$, to satisfy the equations (23).

The mathematics used in this article is developed from the paraunitary transfer function condition (14), which is rearranged to obtain (17). Because the sum-of-products expression (17) is equal to 1, and only the product $C_{00} z_1^0 z_2^0$ is not a complex number, C_{00} has to be equal to 1. All of the remaining $C_{kl} z_1^k z_2^l$ products are complex numbers, and therefore all C_{kl} have to be equal to 0. This results in one expression that equates the left-hand side to 1, and the rest of the equations are equal to 0, respectively.

One additional transfer function G_1 described by (12) gives $m = N_1 N_2 + (N_1 - 1)(N_2 - 1)$ equations

in the set of equations (21) with $N_1 N_2$ variables. Another additional transfer function G_2 described by (12) gives the same number of equations in the set of equations (21) but doubles the number of variables to $n = 2N_1 N_2$. Now, the number of variables is greater than the number of equations. This means that two transfer functions $G_1(z_1, z_2)$ and $G_2(z_1, z_2)$ are sufficient to solve the set of equations (21) and hence

$$N_p = 2. \qquad (24)$$

Now, (14) can be expressed as follows:

$$\mathbf{H}^{\mathrm{T}}\left(z_1^{-1}, z_2^{-1}\right) \mathbf{H}\left(z_1, z_2\right)$$
$$= \begin{bmatrix} H(z_1^{-1}, z_2^{-1}) \\ G_1(z_1^{-1}, z_2^{-1}) \\ G_2(z_1^{-1}, z_2^{-1}) \end{bmatrix}^{\mathrm{T}} \begin{bmatrix} H(z_1, z_2) \\ G_1(z_1, z_2) \\ G_2(z_1, z_2) \end{bmatrix} = 1, \qquad (25)$$

and due to the power complementary property of the paraunitary all-pass FIR filter, (15) can be rearranged into the following expression:

$$|H(e^{j\omega_1}, e^{j\omega_2})|^2 + |G_1(e^{j\omega_1}, e^{j\omega_2})|^2$$
$$+ |G_2(e^{j\omega_1}, e^{j\omega_2})|^2 = 1. \qquad (26)$$

4. Solution of the set of non-linear equations

A modified Newton's method was used to solve the system of non-linear equations (21). The equations in the system (21) are ordered as follows: for each $l = N_2 - 1$ to 1, k changes from $N_1 - 1$ to $-N_1 + 1$, and for $l = 0$, k changes from $N_1 - 1$ to 0. The equations can be described in the vector form

$$\mathbf{C} = \mathbf{Y}, \qquad (27)$$

where the vectors

$$\mathbf{C} = [C_{N_1-1 \ N_2-1} \ \cdots \ C_{-N_1+1 \ N_2-1} \cdots$$
$$C_{N_1-1 \ 1} \ \cdots \ C_{-N_1+1 \ 1} \ \cdots \ C_{N_1-1 \ 0} \ \cdots \ C_{0 \ 0}]^{\mathrm{T}},$$
$$\mathbf{Y} = [0 \ 0 \ \cdots \ 1]^{\mathrm{T}}$$

describe the left and right-hand sides of (21), respectively. The vectors $\mathbf{C}$ and $\mathbf{Y}$ consist of $2N_1 N_2 + (N_1-1)(N_2-1)$ elements.

Equation (27) can be rearranged into the following form:

$$\mathbf{F} = \mathbf{C} - \mathbf{Y} = \mathbf{0}. \qquad (28)$$

The vector $\mathbf{C}$ can be expressed as follows:

$$\mathbf{C} = \mathbf{C}_H + \mathbf{C}_{G_1} + \mathbf{C}_{G_2}, \qquad (29)$$

where the indices denote products of $\mathbf{C}$ dependent on the transfer functions H, G_1, and G_2, respectively. The elements of the transfer function matrix $\mathbf{H}$ are defined,

but the elements g_{1kl} and g_{2kl} for $l = N_2 - 1$ to 0 and $k = N_1 - 1$ to 0 of the transfer function matrices $\mathbf{G}_1$ and $\mathbf{G}_2$ have to be found. Therefore, $\mathbf{F}$ in (28) consists of $m = N_1 N_2 + (N_1 - 1)(N_2 - 1)$ equations with $n = 2N_1 N_2$ variables and can be expressed as follows:

$$\mathbf{F} = [f_1 \ f_2 \ \cdots \ f_i \ \cdots \ f_m]^{\mathrm{T}} = \mathbf{0}, \qquad (30)$$

where

$$f_i(\mathbf{G}_1, \mathbf{G}_2) = C_{Hi} + C_{G_1 i} + C_{G_2 i} - Y_i$$
$$= f_i(g_{1 \ N_1-1 \ N_2-1}, \ g_{1 \ N_1-2 \ N_2-1}, \ \cdots,$$
$$g_{1 \ 0 \ N_2-1}, \ \cdots, g_{1 \ N_1-1 \ 0}, \ \cdots, g_{100},$$
$$g_{2 \ N_1-2 \ N_2-2}, g_{2 \ N_1-3 \ N_2-2}, \ \cdots,$$
$$g_{2 \ 0 \ N_2-2}, \cdots, \ g_{2 \ N_2-2 \ 0}, \ \cdots, \ g_{200}) = 0$$

for $i = 1, 2, \ldots, m$.

Each function $f_i(\mathbf{G}_1, \mathbf{G}_2)$ for $i = 1, 2, \ldots, m$ is a function of $n = 2N_1 N_2$ elements g_{1kl} and g_{2kl} for $l = N_2 - 1$ to 0 and $k = N_1 - 1$ to 0. The set of equations (30) can be expressed in a compact form as

$$\mathbf{F}(\mathbf{x}) = \mathbf{0}, \qquad (31)$$

where

$$\mathbf{x}(\mathbf{G}_1, \mathbf{G}_2) = [x_1 \ x_2 \ \cdots \ x_{N_1 N_2} \ \cdots \ x_{2N_1 N_2}]^{\mathrm{T}}$$
$$[g_{1 \ N_1-1 \ N_2-1} \ g_{1 \ N_1-2 \ N_2-1} \ \cdots$$
$$g_{1 \ 0 \ N_2-1} \ \cdots \ g_{1 \ N_1-1 \ 0} \ \cdots \ g_{100}$$
$$g_{2 \ N_1-2 \ N_2-2} \ g_{2 \ N_1-3 \ N_2-2} \ \cdots$$
$$g_{2 \ 0 \ N_2-2} \ \cdots \ g_{2 \ N_2-2 \ 0} \ \cdots \ g_{200}]^{\mathrm{T}}.$$

Newton's method (Golub and Loan, 1996), which can be written as

$$\mathbf{x}_{i+1} = \mathbf{x}_i - [\mathbf{J}(\mathbf{x_i})]^{-1}\mathbf{F}(\mathbf{x_i}), \qquad (32)$$

where $\mathbf{J}(\mathbf{x})$ is a Jacobi matrix given by

$$\mathbf{J}(\mathbf{x}) = \begin{bmatrix} \frac{\partial f_1(x)}{\partial x_1} & \frac{\partial f_1(x)}{\partial x_2} & \cdots & \frac{\partial f_1(x)}{\partial x_n} \\ \frac{\partial f_2(x)}{\partial x_1} & \frac{\partial f_2(x)}{\partial x_2} & \cdots & \frac{\partial f_2(x)}{\partial x_n} \\ \vdots & \vdots & & \vdots \\ \frac{\partial f_{m-1}(x)}{\partial x_1} & \frac{\partial f_{m-1}(x)}{\partial x_2} & \cdots & \frac{\partial f_{m-1}(x)}{\partial x_n} \\ \frac{\partial f_m(x)}{\partial x_1} & \frac{\partial f_m(x)}{\partial x_2} & \cdots & \frac{\partial f_m(x)}{\partial x_n} \end{bmatrix}, \qquad (33)$$

was used to solve (31) with the accuracy eps:

$$e = |\mathrm{MEAN}[\mathbf{x}_{i+1} - \mathbf{x}_i]| \le eps. \qquad (34)$$

According to the notation presented in (30) and (31), the partial derivatives of $f_i(\mathbf{x})$ with respect to the variables from the matrices $\mathbf{G}_1$ and $\mathbf{G}_2$ are expressed as follows:

for $(-N_1 + 1 \le k \le N_1 - 1$ and $1 \le l \le N_2 - 1)$
or $(0 \le k \le N_1 - 1$ and $l = 0)$

$$\frac{\partial C_{kl}}{\partial g_{1ij}} = \begin{cases} g_{1\ k+i\ l+j} & \text{for } 0 \leq i \leq N_1 - 1 \\ & \text{and } -k \leq i \leq N_1 - 1 - k \\ & \text{and } 0 \leq j \leq N_2 - 1 - l, \\ 0 & \text{otherwise,} \end{cases}$$

$$+ \begin{cases} g_{1\ -k+i\ -l+j} & \text{for } 0 \leq i \leq N_1 - 1 \\ & \text{and } k \leq i \leq N_1 - 1 + k \\ & \text{and } l \leq j \leq N_2 - 1 - l, \\ 0 & \text{otherwise,} \end{cases}$$

(35)

$$\frac{\partial C_{kl}}{\partial g_{2ij}} = \begin{cases} g_{2\ k+i\ l+j} & \text{for } 0 \leq i \leq N_1 - 1 \\ & \text{and } -k \leq i \leq N_1 - 1 - k \\ & \text{and } 0 \leq j \leq N_2 - 1 - l, \\ 0 & \text{otherwise,} \end{cases}$$

$$+ \begin{cases} g_{2\ -k+i\ -l+j} & \text{for } 0 \leq i \leq N_1 - 1 \\ & \text{and } k \leq i \leq N_1 - 1 + k \\ & \text{and } l \leq j \leq N_2 - 1 - l, \\ 0 & \text{otherwise.} \end{cases}$$

(36)

Equation (32) generally requires a non-square system of non-linear equations to be solved. Newton's method was chosen. The method has quadratic convergence. To ensure convergence, the starting point $\mathbf{x}_0$ should be close to the solution. Therefore, the method is usually modified before it is applied to points far from the solution. In order to obtain a good starting vector, a modification of (32) was introduced for $i = 0$. It was proposed by Luenbergerand and Ye (2008). It involves inserting the unit matrix $\mathbf{I}$ into (32) instead of $[\mathbf{J}(\mathbf{x}_i)]^{-1}$ and inserting $\mathbf{C}_{G_1} + \mathbf{C}_{G_2} = 0$ into (29) to determine the starting point $\mathbf{x}_0$.

5. 2-D lossless FIR filter design

2-D FIR filters have many applications in image processing. Using the synthesis of the paraunitary transfer function matrix presented in this article, these filters can be implemented in a lossless system. Some different examples of 2-D FIR filters are used to demonstrate the method described in this article. The coefficients h_{ij} of the matrix $\mathbf{H}$ are given *a priori*, which is common in image processing methods. This matrix is called a kernel or a mask. In all presented examples, the filter mask size is 5×5, filter coefficient values are rounded to four decimal places, and the stopping criterion for Newton's method (34) is

$$e = |\text{MEAN}[\mathbf{x}_{i+1} - \mathbf{x}_i]| \leq 1 \cdot 10^{-7}. \quad (37)$$

The stopping criterion (37) is determined from the accuracy criteria for the state spaces in the paraunitary matrix calculation methods for obtaining a lossless system proposed by Piekarski and Wirski (2005) as well as Wirski and Wawryn (2008).

To specify the starting point $\mathbf{x}_0$, the unit matrix $\mathbf{I}$ is used in (32) instead of $[\mathbf{J}(\mathbf{x}_i)]^{-1}$. The presented examples demonstrate different image processing applications,

including edge detection and blurring or sharpening an image. The applied filter masks have different types of symmetry or no symmetry. In order to verify each obtained lossless FIR filter system, the characteristics of $|H(e^{j\omega_1}, e^{j\omega_2})|$, $|H(e^{j\omega_1}, e^{j\omega_2})|^2$, and $|G_1(e^{j\omega_1}, e^{j\omega_2})|^2 + |G_2(e^{j\omega_1}, e^{j\omega_2})|^2$ are plotted in one figure. They should illustrate that the power complementary property of the lossless filter described by (26) is satisfied.

The number of iterations depends on each individual case, and therefore it is not possible to estimate the complexity of the calculations. However, it is possible to estimate the complexity of an individual iteration. It is assumed that the computational complexity is determined on the basis of the number of time-consuming operations, i.e., multiplication and division operations. The functions $f_1, \ldots, f_m$ (30) and Newton's method (32) contain the most time-consuming operations. The calculation of the inverse Jacobi matrix has the largest number of operations. Assuming an $n \times n$ square matrix for simplicity, the computational complexity (in O-notation) is no greater than $O(n^3)$ (Cormen *et al.*, 2009; Brent and Zimmermann, 2010). All other operations are of lower complexity; matrix-vector multiplication has a complexity of $O(n^2)$. Since $n < m$, by assuming n-based complexities, we also consider the most pessimistic case. Assuming the most common situation, where $N_1 = N_2 = N$, we have $n = 2N^2$, so for the determination of the inverse matrix, the complexity can be defined as $O(N^6)$, where N is compatible with (5) and (9). As already mentioned, the other operations are of lower complexity, so they can be omitted.

5.1. Example 1: A high-pass sharpening filter with octagonal symmetry.
The matrix $\mathbf{H}$ (5) is given as the following mask:

$$\mathbf{H} = \begin{bmatrix} 0 & -1 & -1 & -1 & 0 \\ -1 & 2 & -4 & 2 & -1 \\ -1 & -4 & 13 & -4 & -1 \\ -1 & 2 & -4 & 2 & -1 \\ 0 & -1 & -1 & -1 & 0 \end{bmatrix} \frac{1}{H_{\text{MAX}}}, \quad (38)$$

and according to (3), $H_{\text{MAX}} = 43$. The starting point for $i = 0$ (Luenbergerand and Ye, 2008) is equal to

$$\begin{aligned}
\mathbf{x}_0 = [&0\ 0\ 0.0005\ 0.0011\ 0.0016\ 0.0011\ 0.0005 \\
&0\ 0\ 0\ 0.0011\ -0.0011\ 0.0032\ 0\ 0.0032 \\
&-0.0011\ 0.0011\ 0\ 0\ 0.0005\ -0.0011 \\
&0.0119\ -0.0195\ 0.0087\ -0.0195 \\
&0.0119\ -0.0011\ 0.0005\ 0.0011\ 0.0032 \\
&-0.0195\ 0.0508\ -0.0714\ 0.0508 \\
&-0.0195\ 0.0032\ 0.0011\ 0.0016\ 0\ 0.0087 \\
&-0.0714\ 0.1412\ 0\ 0\ 0\ 0\ 0\ 0\ 0\ 0].
\end{aligned} \quad (39)$$

For the first iteration, (30) is

$$
\begin{aligned}
\mathbf{F} = [&0\ 0\ 0.0006\ -0.0026\ 0.0019\ -0.01 \\
&0.001\ -0.0028\ 0\ 0\ 0.0011 \\
&-0.0012\ 0.0088\ -0.0018\ 0.006 \\
&-0.0039\ 0.0015\ 0\ 0.0005 \\
&-0.0011\ 0.0119\ -0.0238\ 0.0134 \\
&-0.0206\ 0.0192\ -0.0009\ 0.0005 \\
&0.0011\ 0.0032\ -0.0198\ 0.0529 \\
&-0.0812\ 0.0516\ -0.0299\ 0.0033 \\
\\
&0.001\ 0.0016\ -0.0002\ 0.0174 \\
&-0.0719\ -0.8215],
\end{aligned}
\tag{40}
$$

and from (32), the following can be obtained:

$$
\begin{aligned}
\mathbf{x}_1 = [&0.0653\ -0.0976\ -0.8662\ -1.9908 \\
&-0.5184\ -4.5931\ 5.4283\ 4.3785 \\
&-2.4232\ 10.593\ 9.5398\ -6.0711 \\
&-16.7465\ -2.5802\ -4.044\ 0.772 \\
\\
&-6.4239\ -4.523\ 6.8549\ -1.8654 \\
&11.1141\ 15.7006\ -37.4942\ -9.1179 \\
&13.1047\ -0.8381\ 1.6732\ -0.5466 \\
&2.815\ -0.7825\ 1.7605\ -4.2803 \\
&3.2877\ -0.3992\ 0.0087\ -2.4599 \\
&-1.8226\ 6.5851\ 1.0076\ 1.2389 \\
&1.1363\ 7.7589\ 6.5491\ 2.8655 \\
&-3.7485\ 0.6084\ 1.33\ -0.4292 \\
&-1.8901\ 0.718].
\end{aligned}
\tag{41}
$$

To satisfy (37), 22 iterations were executed and the following matrices were obtained:

$\mathbf{G}_1$

$$
= \begin{bmatrix}
0.0506 & -0.0696 & -0.0642 & -0.0122 & -0.0006 \\
0.2754 & -0.1192 & 0.0085 & -0.0247 & -0.0054 \\
-0.4636 & -0.3916 & -0.0191 & 0.0037 & -0.0076 \\
-0.0337 & -0.0990 & -0.0337 & -0.0041 & -0.0024 \\
0.1297 & -0.0546 & 0.0054 & -0.0038 & -0.0005
\end{bmatrix},
\tag{42}
$$

$\mathbf{G}_2$

$$
= \begin{bmatrix}
-0.0058 & -0.0422 & 0.2770 & 0.1335 & 0.0080 \\
-0.0591 & -0.0636 & 0.2608 & -0.2150 & 0.0669 \\
-0.0425 & -0.2262 & 0.2200 & 0.0909 & -0.0091 \\
0.0063 & 0.0183 & -0.1390 & 0.0254 & -0.0008 \\
0.0095 & 0.0360 & -0.0381 & 0.0035 & -0.0043
\end{bmatrix}.
\tag{43}
$$

The amplitude characteristics of $|H(e^{j\omega_1}, e^{j\omega_2})|$, $|H(e^{j\omega_1}, e^{j\omega_2})|^2$, $|G_1(e^{j\omega_1}, e^{j\omega_2})|^2 + |G_2(e^{j\omega_1}, e^{j\omega_2})|^2$ are presented in Fig. 2.

5.2. Example 2: A low-pass smoothing filter with quadrantal symmetry. A 2-D blurring FIR filter can be composed of two 1-D FIR filters, and the matrix $\mathbf{H}$ from the transfer function (5) is of the form

$$
\mathbf{H} = \mathbf{H}_v \mathbf{H}_h =
\begin{bmatrix} 0.0096 \\ 0.2054 \\ 0.5699 \\ 0.2054 \\ 0.0096 \end{bmatrix}
\begin{bmatrix} 0.0375 \\ 0.2391 \\ 0.4433 \\ 0.2391 \\ 0.0375 \end{bmatrix}^{\mathrm{T}}
$$

$$
= \begin{bmatrix}
0.0004 & 0.0023 & 0.0043 & 0.0023 & 0.0004 \\
0.0077 & 0.0491 & 0.0911 & 0.0491 & 0.0077 \\
0.0214 & 0.1363 & 0.2526 & 0.1363 & 0.0214 \\
0.0077 & 0.0491 & 0.0911 & 0.0491 & 0.0077 \\
0.0004 & 0.0023 & 0.0043 & 0.0023 & 0.0004
\end{bmatrix},
\tag{44}
$$

where $\mathbf{H}_v$ and $\mathbf{H}_h$ are the coefficient vectors of two 1-D filters for vertical and horizontal processing, respectively. For $\mathbf{H} = \mathbf{H}_v \mathbf{H}_h$, two different filters can be specified for processing in both directions.

The starting point for $i = 0$ (Luenbergerand and Ye, 2008) is equal to

$$
\begin{aligned}
\mathbf{x}_0 = [&0\ 0\ 0\ 0\ 0\ 0\ 0\ 0\ 0\ 0\ 0.0001\ 0.0004 \\
&0.0009\ 0.0012\ 0.0009\ 0.0004\ 0.0001 \\
&0\ 0.0001\ 0.0010\ 0.0048\ 0.0122\ 0.0167 \\
&0.0122\ 0.0048\ 0.0010\ 0.0001\ 0.0003 \\
&0.0043\ 0.0215\ 0.0547\ 0.0747\ 0.0547 \\
&0.0215\ 0.0043\ 0.0003\ 0.0006\ 0.0073 \\
&0.0370\ 0.0941\ 0.1284\ 0\ 0\ 0\ 0\ 0\ 0\ 0\ 0\ 0].
\end{aligned}
\tag{45}
$$

To satisfy (37), 28 iterations were executed and the following matrices were obtained:

$\mathbf{G}_1$

$$
= \begin{bmatrix}
0.0669 & -0.1169 & 0.0257 & -0.0223 & 0.0179 \\
-0.0321 & 0.0484 & -0.2868 & 0.2395 & 0.0369 \\
0.1805 & 0.0025 & 0.3217 & 0.0717 & -0.0608 \\
0.0550 & -0.3812 & -0.0961 & 0.0561 & 0.0342 \\
-0.0012 & -0.0398 & -0.0380 & -0.0872 & -0.0335
\end{bmatrix},
\tag{46}
$$

$\mathbf{G}_2$

$$
= \begin{bmatrix}
-0.0720 & -0.1556 & 0.0217 & -0.0055 & 0.0284 \\
0.0109 & -0.1993 & -0.0374 & 0.4062 & 0.0589 \\
-0.1154 & 0.0459 & -0.0728 & -0.0297 & -0.0983 \\
-0.0348 & 0.2746 & -0.1885 & 0.0154 & 0.0421 \\
0.0007 & 0.0242 & -0.0025 & 0.0405 & -0.0311
\end{bmatrix}.
\tag{47}
$$

The amplitude characteristics of $|H(e^{j\omega_1}, e^{j\omega_2})|$, $|H(e^{j\omega_1}, e^{j\omega_2})|^2$, $|G_1(e^{j\omega_1}, e^{j\omega_2})|^2 + |G_2(e^{j\omega_1}, e^{j\omega_2})|^2$ are presented in Fig. 3.
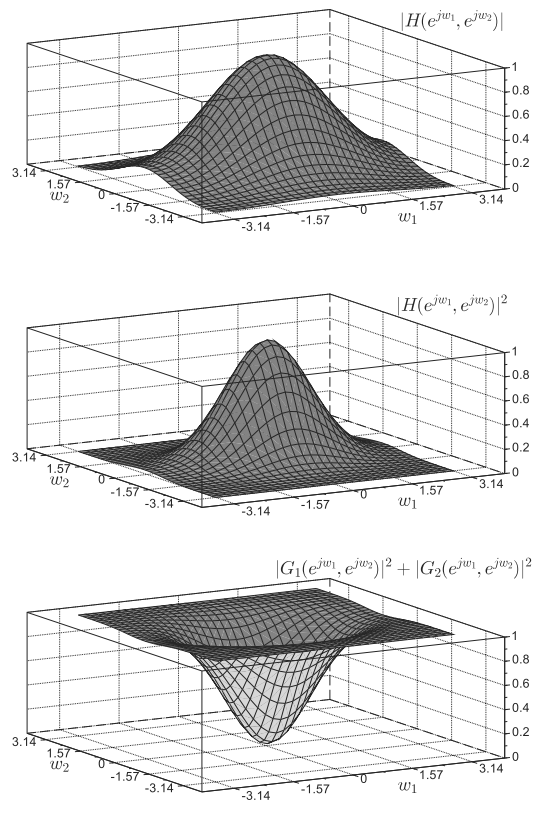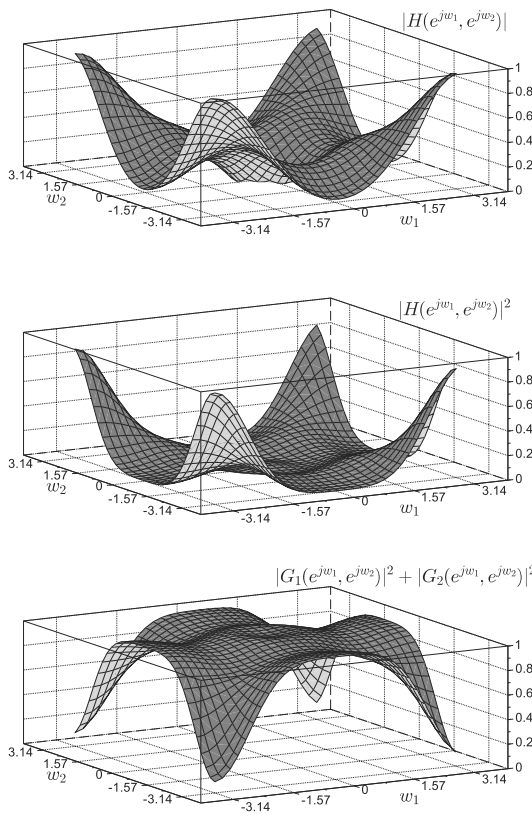
Fig. 2. High-pass sharpening filter with octagonal symmetry: amplitude characteristics of $|H(e^{j\omega_1}, e^{j\omega_2})|$, $|H(e^{j\omega_1}, e^{j\omega_2})|^2$, $|G_1(e^{j\omega_1}, e^{j\omega_2})|^2 + |G_2(e^{j\omega_1}, e^{j\omega_2})|^2$.

Fig. 3. Low-pass smoothing filter with quadrantal symmetry: amplitude characteristics of $|H(e^{j\omega_1}, e^{j\omega_2})|$, $|H(e^{j\omega_1}, e^{j\omega_2})|^2$, $|G_1(e^{j\omega_1}, e^{j\omega_2})|^2 + |G_2(e^{j\omega_1}, e^{j\omega_2})|^2$.

5.3. Example 3: An emboss filter that is centrally antisymmetric.

The matrix $\mathbf{H}$ (5) is given as the following mask:

$$\mathbf{H} = \begin{bmatrix} 1 & 0 & 0 & 0 & 0 \\ 0 & 1 & 0 & 0 & 0 \\ 0 & 0 & 0 & 0 & 0 \\ 0 & 0 & 0 & -1 & 0 \\ 0 & 0 & 0 & 0 & -1 \end{bmatrix} \frac{1}{H_{\text{MAX}}}, \qquad (48)$$

and according to (3), $H_{\text{MAX}} = 4$. The starting point for $i = 0$ (Luenbergerand and Ye, 2008) is equal to

$$\begin{aligned} \mathbf{x}_0 = [&-0.0625\,0\,0\,0\,0\,0\,0\,0\,0\,0 \\ &-0.1250\,0\,0\,0\,0\,0\,0\,0\,0\,0 \\ &-0.0625\,0\,0\,0\,0\,0\,0\,0\,0\,0 \\ &0.1250\,0\,0\,0\,0\,0\,0\,0\,0\,0 \\ &0.2500\,0\,0\,0\,0\,0\,0\,0\,0\,0]. \end{aligned} \qquad (49)$$

To satisfy (37), 13 iterations were executed and the

following matrices were obtained:

$$\mathbf{G}_1$$
$$= \begin{bmatrix} -0.3154 & 0.0005 & 0.1911 & 0.0078 & 0.0001 \\ -00174 & -0.0602 & -0.0060 & -0.1083 & -0.0005 \\ -0.1744 & -0.0099 & -0.0379 & -0.0050 & -0.0118 \\ 0.0024 & 0.0987 & 0.0018 & 0.0114 & 0.0144 \\ -0.0883 & 0.0078 & -0.2790 & -0.0007 & -0.1982 \end{bmatrix},$$
$$(50)$$

$$\mathbf{G}_2$$
$$= \begin{bmatrix} -0.0020 & 0.1822 & -0.0070 & 0.0690 & 0.0006 \\ -0.3530 & 0.0083 & -0.1424 & -0.0049 & 0.0063 \\ 0.0085 & -0.1874 & -0.0030 & 0.1089 & -0.0032 \\ -0.1607 & -0.0011 & 0.1666 & 0.0029 & 0.1077 \\ 0.0079 & 0.2447 & 0.0170 & -0.2749 & 0.0037 \end{bmatrix}.$$
$$(51)$$

The amplitude characteristics of $|H(e^{j\omega_1}, e^{j\omega_2})|$, $|H(e^{j\omega_1}, e^{j\omega_2})|^2$, $|G_1(e^{j\omega_1}, e^{j\omega_2})|^2 + |G_2(e^{j\omega_1}, e^{j\omega_2})|^2$ are presented in Fig. 4.

5.4. Example 4: A Kirsch vertical edge detection filter without symmetry that is antisymmetric.
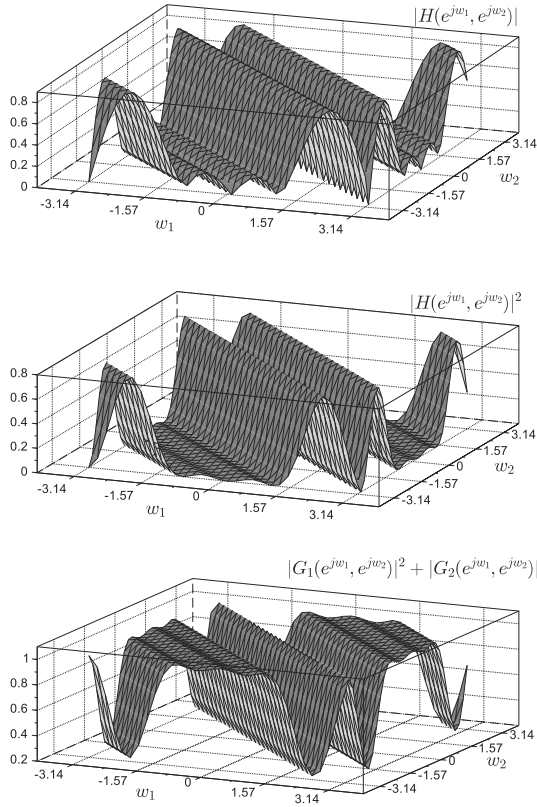
The matrix

Fig. 4. Emboss filter that is centrally antisymmetric: amplitude characteristics of $|H(e^{j\omega_1}, e^{j\omega_2})|$, $|H(e^{j\omega_1}, e^{j\omega_2})|^2$, and $|G_1(e^{j\omega_1}, e^{j\omega_2})|^2 + |G_2(e^{j\omega_1}, e^{j\omega_2})|^2$.
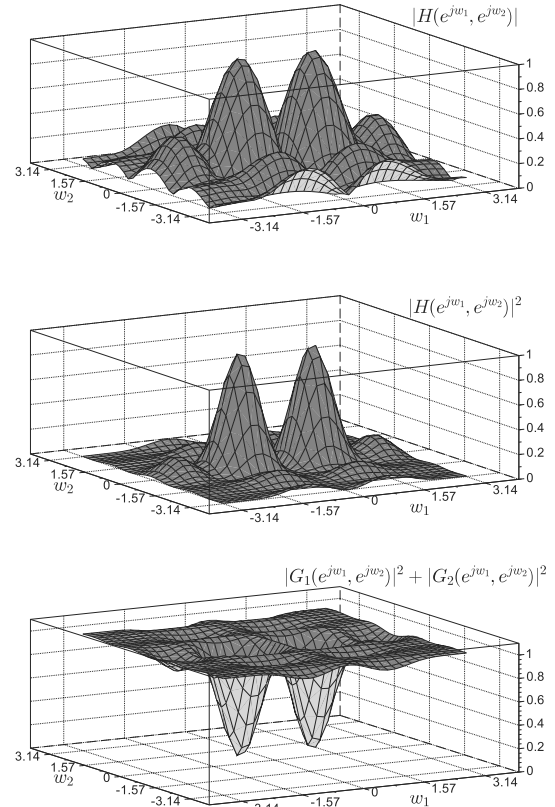
Fig. 5. Kirsch vertical edge detection filter without symmetry that is antisymmetric: amplitude characteristics of $|H(e^{j\omega_1}, e^{j\omega_2})|$, $|H(e^{j\omega_1}, e^{j\omega_2})|^2$, and $|G_1(e^{j\omega_1}, e^{j\omega_2})|^2 + |G_2(e^{j\omega_1}, e^{j\omega_2})|^2$.

H (5) is given as the following mask:

$$\mathbf{H} = \begin{bmatrix} 9 & 9 & 9 & 9 & 9 \\ 9 & 5 & 5 & 5 & 9 \\ -7 & -3 & 0 & -3 & -7 \\ -7 & -3 & -3 & -3 & -7 \\ -7 & -7 & -7 & -7 & -7 \end{bmatrix} \frac{1}{H_{\mathrm{MAX}}}, \qquad (52)$$

and according to (3), $H_{\mathrm{MAX}} = 126$. The starting point for $i = 0$ (Luenbergerand and Ye, 2008) is equal to

$$\mathbf{x}_0 = [\,-0.0040 \; -0.0079 \; -0.0119 \; -0.0159$$
$$-0.0198 \; -0.0159 \; -0.0119 \; -0.0079$$
$$-0.0040 \; -0.0079 \; -0.0118 \; -0.0157$$

$$-0.0197 \; -0.0276 \; -0.0197 \; -0.0157$$
$$-0.0118 \; -0.0079 \; -0.0049 \; -0.0052$$
$$-0.0061 \; -0.0074 \; -0.0133 \; -0.0074$$
$$-0.0061 \; -0.0052 \; -0.0049 \; 0.0073 \qquad (53)$$
$$0.0111 \; 0.0152 \; 0.0190 \; 0.0263 \; 0.0190$$
$$0.0152 \; 0.0111 \; 0.0073 \; 0.0195 \; 0.0273$$
$$0.0356 \; 0.0480 \; 0.0711 \; 0 \; 0 \; 0 \; 0 \; 0 \; 0 \; 0 \; 0].$$

To satisfy (37), 13 iterations were executed and the following matrices were obtained:

$\mathbf{G}_1$
$$= \begin{bmatrix} -0.0913 & 0.0483 & -0.0663 & -0.0735 & -0.0666 \\ -0.2233 & 0.1000 & -0.1800 & 0.2245 & 0.0440 \\ -0.2757 & 0.0977 & 0.2632 & 0.0108 & 0.0133 \\ -0.1676 & -0.2100 & 0.1911 & 0.1112 & 0.0198 \\ -0.0299 & 0.0542 & -0.1138 & -0.1131 & -0.0443 \end{bmatrix},$$
$$(54)$$

$\mathbf{G}_2$
$$= \begin{bmatrix} 0.0137 & 0.0582 & -0.0734 & 0.0533 & 0.0178 \\ 0.0227 & 0.0592 & 0.2037 & -0.0089 & -0.0267 \\ 0.1465 & 0.0655 & -0.1254 & 0.2747 & -0.0612 \\ 0.0586 & -0.4018 & 0.0274 & 0.0356 & -0.0013 \\ 0.1110 & 0.1928 & 0.2358 & 0.0066 & -0.0059 \end{bmatrix}.$$
$$(55)$$

The amplitude characteristics of $|H(e^{j\omega_1}, e^{j\omega_2})|$, $|H(e^{j\omega_1}, e^{j\omega_2})|^2$, $|G_1(e^{j\omega_1}, e^{j\omega_2})|^2 + |G_2(e^{j\omega_1}, e^{j\omega_2})|^2$ are presented in Fig. 5.

In all the examples presented above, the coefficients h_{ij} of the matrix **H** of the 2-D FIR filter are given *a priori*. If they are not given, then the Fourier series can be used to calculate the coefficients h_{ij} of the matrix

H. The frequency response of the filter is given by (Charalambous, 1985)

$$
H(e^{-j\omega_1}, e^{-j\omega_2}) = e^{-j[(N_1-1)\omega_1+(N_2-1)\omega_2)]}
$$
$$
\times \sum_{k=0}^{N_1-1} \sum_{l=0}^{N_2-1} h_{kl} \cos k\omega_1 \cos l\omega_2. \tag{56}
$$

If quadrantal symmetry in the 2-D constant-phase FIR filter is desired, then additional conditions (7) and (8) hold (Charalambous, 1985). With respect to (56) and (6), the coefficients h_{kl} in the rectangle $k = 0, 1, \ldots, n_1$ and $l = 0, 1, \ldots, n_2$ are sufficient to describe the frequency response of the filter, as shown in Fig. 6. The frequency response (56) of the filter with a constant phase delay and quadrantal symmetry (Charalambous, 1985) can be expressed in the following form:

$$
H(e^{-j\omega_1}, e^{-j\omega_2})
$$
$$
= e^{-j(n_1\omega_1+n_2\omega_2)} \sum_{k=0}^{n_1} \sum_{l=0}^{n_2} a_{kl} \cos k\omega_1 \cos l\omega_2, \tag{57}
$$

where

$$
\begin{aligned}
a_{0,0} &= h_{n_1,n_2}, \\
a_{k,0} &= 2h_{n_1-k,n_2} && \text{for } 1 \le k \le n_1, \\
a_{0,l} &= 2h_{n_1,n_2-l} && \text{for } 1 \le l \le n_2, \\
a_{k,l} &= 4h_{n_1-k,\,n_2-l} && \text{for } 1 \le k \le n_1,\ 1 \le l \le n_2,
\end{aligned} \tag{58}
$$

n_1 and n_2 are described by (6).

If octagonal symmetry in the 2-D constant phase FIR filter is also desired, then additional conditions (9) and (10) hold. With respect to (56), (6), and $n_1 = n_2 = n$, the coefficients h_{kl} in the triangle $k = 0, 1, \ldots, n$ and $l = 0, 1, \ldots, n$ are sufficient to describe the frequency response of the filter, as shown in Fig. 7. The frequency response (56) of the filter with a constant phase delay and octagonal symmetry can be expressed in the following form:

$$
H(e^{-j\omega_1}, e^{-j\omega_2})
$$
$$
= e^{-jn(\omega_1+\omega_2)} \sum_{k=0}^{n} \sum_{l=0}^{n} a_{kl} \cos k\omega_1 \cos l\omega_2, \tag{59}
$$

where

$$
\begin{aligned}
a_{0,0} &= h_{n,n}, \\
a_{k,k} &= 4h_{n-k,n-k} && \text{for } 1 \le k \le n, \\
a_{k,0} &= 4h_{n-k,n} && \text{for } 1 \le k \le n, \\
a_{k,l} &= 8h_{n-k,n-l} && \text{for } 2 \le k \le n,\ 1 \le l \le k-1.
\end{aligned} \tag{60}
$$

The coefficients h_{kl} can be found using an approximation of the 2-D FIR filter transfer function (56). The 2-D FIR filter transfer functions (58) and (60) and the coefficients
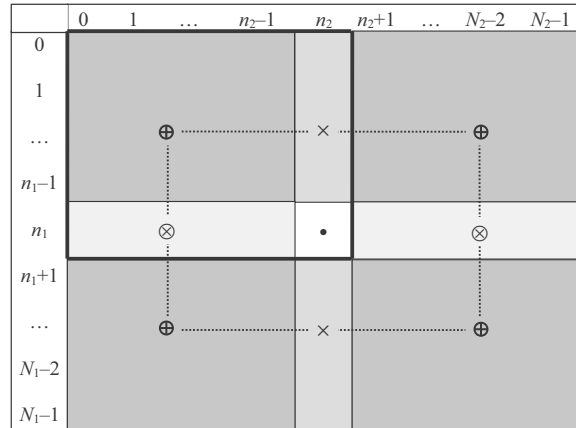

Fig. 6. Locations of the $(n_1 + 1)(n_2 + 1)$ h_{kl} coefficients used for the calculations expressed by (57) and (58) are inside the rectangle marked with a thick line.
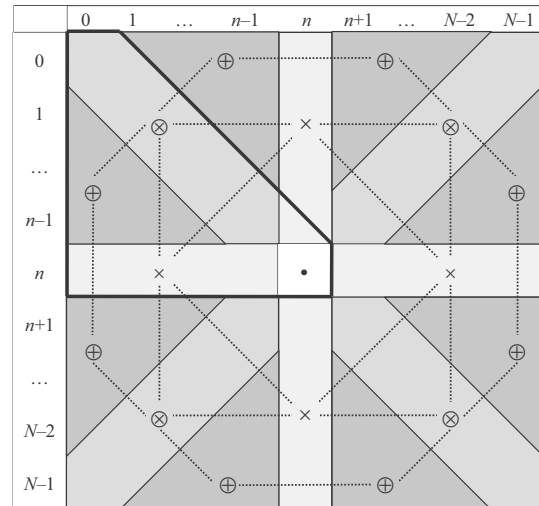

Fig. 7. Locations of the $\frac{(n+1)(n+1)}{2}$ h_{kl} coefficients used for the calculations expressed by (59) and (60) are inside the triangle marked with a thick line.

a_{kl} can be found using an approximation, and then they can be used to find the coefficients h_{ij}.

The desired amplitude response $A(\omega_1, \omega_2)$ of a 2-D FIR filter is usually given by m amplitude discrete values $A_i(\omega_{1_i}, \omega_{2_i})$, where $i = 1, \ldots, m$. The approximation of the 2-D FIR filter transfer function satisfying the desired specifications may be performed using several methods. A weighted least-squares method and a minimax method are among the methods that are most often used (Lu, 2002). If $W(\omega_1, \omega_2)$ is the weighted function in the weighted least squares method, then the coefficients a_{kl} (58) can be obtained by minimizing (Mitra and Kaiser, 1993)

$$
E = \sum_{i=1}^{m} [W(\omega_{1_i}, \omega_{2_i})\,(H(\omega_{1_i}, \omega_{2_i}) - A(\omega_{1_i}, \omega_{2_i}))]^2. \tag{61}
$$

5.5. Example 5: A low-pass denoising filter from approximation with octagonal symmetry.

A 2-D low-pass filter can be designed to satisfy the amplitude response from Fig. 8 for $\psi_p = 0.34$ and $\psi_a = 0.37$ (ψ_p and ψ_a are the passband and stopband, respectively). The coefficients h_{ij} of the $\mathbf{H}$ matrix (4) are obtained from (5) and (6) with the use of the minimax approximation, and $\mathbf{H}$ is of the form

$$\mathbf{H} = \begin{bmatrix} 0.0425 & 0.0258 & 0.0632 & 0.0258 & 0.0425 \\ 0.0258 & 0.0157 & 0.0384 & 0.0157 & 0.0258 \\ 0.0632 & 0.0384 & 0.0942 & 0.0384 & 0.0632 \\ 0.0258 & 0.0157 & 0.0384 & 0.0157 & 0.0258 \\ 0.0425 & 0.0258 & 0.0632 & 0.0258 & 0.0425 \end{bmatrix}. \tag{62}$$

The starting point for $i = 0$ (Luenbergerand and Ye, 2008) is

$$\begin{aligned} \mathbf{x}_0 = [&0.0018\ 0.0022\ 0.0060\ 0.0055\ 0.0089 \\ &0.0055\ 0.0060\ 0.0022\ 0.0018\ 0.0022 \\ &0.0027\ 0.0073\ 0.0066\ 0.0109\ 0.0066 \\ &0.0073\ 0.0027\ 0.0022\ 0.0060\ 0.0073 \\ &0.0202\ 0.0183\ 0.0299\ 0.0183\ 0.0202 \\ &0.0073\ 0.0060\ 0.0055\ 0.0066\ 0.0183 \\ &0.0165\ 0.0270\ 0.0165\ 0.0183\ 0.0066 \\ &0.0055\ 0.0089\ 0.0109\ 0.0299\ 0.0270 \\ &0.0443\ 0\ 0\ 0\ 0\ 0\ 0\ 0\ 0]. \end{aligned} \tag{63}$$

To satisfy (37), 22 iterations were executed and the following matrices were obtained:

$$\begin{aligned} &\mathbf{G}_1 \\ &= \begin{bmatrix} 0.1330 & 0.0079 & -0.2285 & -0.2271 & -0.0278 \\ 0.0919 & -0.1656 & 0.1305 & 0.1408 & -0.0210 \\ 0.2120 & 0.0383 & 0.0344 & 0.0770 & -0.0299 \\ 0.0766 & 0.1590 & -0.0080 & 0.0473 & -0.0048 \\ 0.1336 & -0.2035 & 0.0004 & -0.0035 & -0.0264 \end{bmatrix}, \end{aligned} \tag{64}$$

$$\begin{aligned} &\mathbf{G}_2 \\ &= \begin{bmatrix} 0.0356 & -0.0743 & -0.1119 & -0.0285 & 0.0482 \\ -0.0067 & -0.1829 & 0.0983 & 0.0927 & 0.0275 \\ 0.0304 & -0.2989 & 0.0378 & 0.0969 & 0.0770 \\ 0.0343 & -0.4162 & 0.0392 & -0.0372 & 0.0335 \\ 0.0396 & 0.4899 & -0.0693 & 0.0573 & 0.0479 \end{bmatrix}. \end{aligned} \tag{65}$$

The amplitude characteristics of $|H(e^{j\omega_1}, e^{j\omega_2})|$, $|H(e^{j\omega_1}, e^{j\omega_2})|^2$, $|G_1(e^{j\omega_1}, e^{j\omega_2})|^2 + |G_2(e^{j\omega_1}, e^{j\omega_2})|^2$ are presented in Fig. 9.

All of the lossless systems obtained in Examples 1–5 satisfy the paraunitary condition (25) and the power complementary property of the paraunitary all-pass FIR filter (26), because the second and third plots of the figures provided for each example show that the sum of the characteristics $|H(e^{j\omega_1}, e^{j\omega_2})|^2$ and $|G_1(e^{j\omega_1}, e^{j\omega_2})|^2 + |G_2(e^{j\omega_1}, e^{j\omega_2})|^2$ is 1.
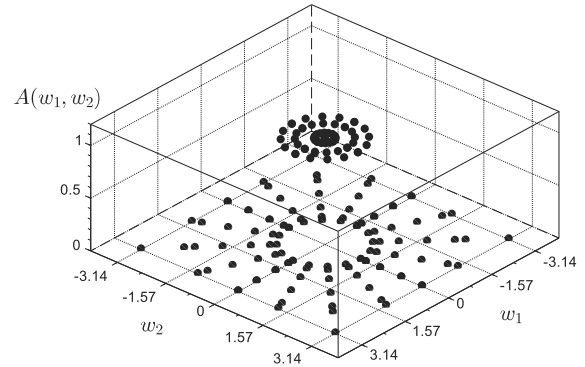

Fig. 8. Sample points of the amplitude response for a 2-D low-pass FIR filter for $\psi_p = 0.34$ and $\psi_a = 0.37$.
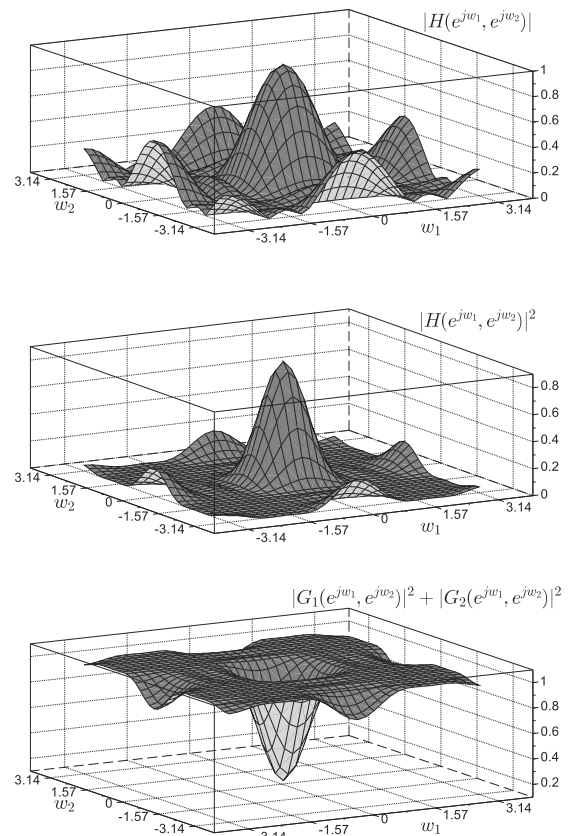

Fig. 9. Low-pass denoising filter from approximation with octagonal symmetry: amplitude characteristics of $|H(e^{j\omega_1}, e^{j\omega_2})|$, $|H(e^{j\omega_1}, e^{j\omega_2})|^2$, and $|G_1(e^{j\omega_1}, e^{j\omega_2})|^2 + |G_2(e^{j\omega_1}, e^{j\omega_2})|^2$.

6. Concluding remarks

The presented method makes it possible to determine the paraunitary transfer function matrices of two-dimensional lossless FIR filters. A modified Newton's method was used to solve the paraunitary conditions of the matrices

described by a set of non-linear equations. As they are often used in image processing, 5×5 kernel filters and 2-D low-pass filters obtained through approximation were used as examples. For all examples, the number of equations was 41 and the number of variables was 25. The modified Newton's method converged with an accuracy of $e = |\text{MEAN}[\mathbf{x}_{i+1} - \mathbf{x}_i]| \leq 1 \cdot 10^{-7}$ and the produced solutions for all presented FIR filters after less than 50 iterations. The obtained matrices of the lossless FIR filters $\mathbf{H}(z_1, z_2)$ have a size of 3×1. This means that they have three outputs, resulting in three transfer functions $H(z_1, z_2)$, $G_1(z_1, z_2)$, and $G_2(z_1, z_2)$ for each output.

A sample image processed by the Kirsch filter (Section 5.4) has been included. The original initial image is shown in Fig. 10(a) and the image processed by the filter $H(z_1, z_2)$ (52) is shown in Fig. 10(b). The typical effect of direction edge filters is visible. The image processed by the filter $G_1(z_1, z_2)$ (54) is shown in Fig. 10(c). Diagonal edges are visible at places where there are strong dynamics among neighbouring pixel values. Figure 10(d) shows the image with blurred details that results from using the $G_2(z_1, z_2)$ filter (55). Additionally, the Scilab code for a 5×5 filter is provided in Appendix.

2-D lossless FIR filters can be implemented in hardware, usually as a direct realisation composed of adders, multipliers, and delay units (Lu, 2002; Antoniou, 2005; Wnuk, 2008). A better realisation consists of delay units and rotators (Givens rotation elements), which are the simplest possible components for orthogonal filtering (Dewilde, 2019; Andraka, 1998; Wawryn *et al.*, 2010; Puchala, 2022). Householder reflectors based on Householder transformations are also possible components that are suitable for orthogonal filter realisation (Puchala, 2022; Anju and Mathurakani, 2016; Brugière *et al.*, 2019). Further work with presented filters may also involve statistical analyses used for harmonic signals (Sienkowski and Krajewski, 2021).

References

Andraka, R. (1998). A survey of CORDIC algorithms for FPGA based computers, *Symposium on Field Programmable Gate Arrays, North Kingstown, USA*, pp. 191–200.

Anju, R.T. and Mathurakani, M. (2016). Realization of hardware architectures for Householder transformation based QR decomposition using Xilinx system generator block sets, *International Journal of Science Technology and Engineering* **2**(8): 202–206.

Antoniou, A. (2005). *Digital Signal Processing: Signals, Systems, and Filters*, McGraw-Hill Education, New York.

Basu, S. and Fettweis, A. (1985). On the factorization of scattering transfer matrices of multidimensional lossless two-ports, *IEEE Transactions on Circuits and Systems* **32**(9): 925–934.

Belevitch, V. (1968). *Classical Network Theory*, Holden-Day, San Francisco.
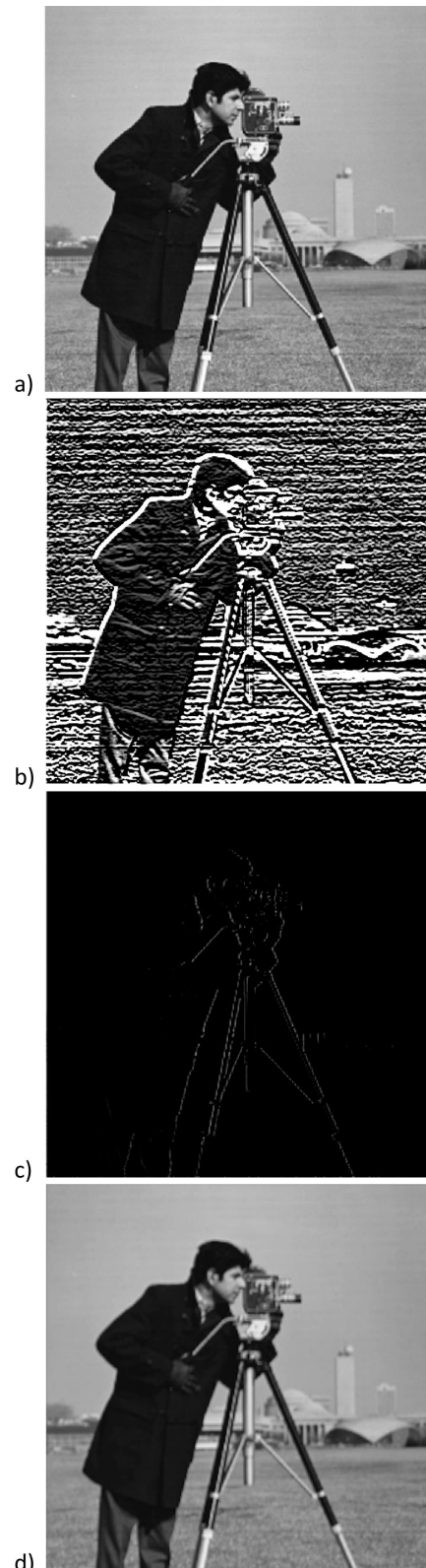
a)

b)

c)

d)

Fig. 10. Example of processing via the paraunitary realization of the Kirsch filter (Section 5.4): original image (a), filtering using $H(z_1, z_2)$ (52) (b), filtering using $G_1(z_1, z_2)$ (54) (c), filtering using $G_2(z_1, z_2)$ (55) (d).

Bose, N.K. and Strintzis, M.G. (1973). A solution to the multivariable matrix factorization problem, *Journal of Engineering Mathematics* **7**: 263–271.

Brent, R.P. and Zimmermann, P. (2010). *Modern Computer Arithmetic*, Cambridge University Press, Cambridge.

Brugière, T., Baboulin, M., Valiron, B. and Allouche, C. (2019). Quantum circuits synthesis using Householder transformations, *Computer Physics Communications* **248**: 107001.

Charalambous, C. (1985). The performance of an algorithm for minimax design of two-dimensional linear phase FIR digital filters, *IEEE Transactions on Circuits and Systems* **32**(10): 1016–1028.

Cormen, T.H., Leiserson, C.E., Rivest, R.L. and Stein, C. (2009). *Introduction to Algorithms, 3rd Edition*, MIT Press, Cambridge.

Deprettere, E. and Dewilde, P. (1980). Orthogonal cascade realization of real multiport digital filters, *International Journal of Circuit Theory and Applications* **8**(3): 245–272.

Dewilde, P. (2019). The power of orthogonal filtering, *IEEE Circuits and Systems Magazine* **18**: 70–C3.

Fettweis, A. (1971). Digital filter structures related to classical filter networks, *Archiv der elektrischen Übertragung: AEÜ* **25**: 79–89.

Fettweis, A. (1982). On the scattering matrix and the scattering transfer matrix of multidimensional lossless two-ports, *Archiv der elektrischen Übertragung: AEÜ* **36**: 374–381.

Fettweis, A. (1991). The role of passivity and losslessness in multidimensional digital signal processing—New challenges, *IEEE International Symposium on Circuits and Systems, Singapore*, Vol. 1, pp. 112–115.

Golub, G. and Loan, C. (1996). *Matrix Computations*, Johns Hopkins University Press, Baltimore.

Kaczorek, T. (2008). The choice of the forms of Lyapunov functions for a positive 2D Roesser model, *International Journal of Applied Mathematics and Computer Science* **17**(4): 471–475, DOI: 10.2478/v10006-007-0039-7.

Kaczorek, T. and Rogowski, K. (2010). Positivity and stabilization of fractional 2D linear systems described by the Roesser model, *International Journal of Applied Mathematics and Computer Science* **20**(1): 85–92, DOI: 10.2478/v10006-010-0006-6.

Liu, Q., Ling, B., Dai, Q., Miao, Q. and Liu, C. (2017). Optimal maximally decimated M-channel mirrored paraunitary linear phase FIR filter bank design via norm relaxed sequential quadratic programming, *Journal of Industrial and Management Optimization* **13**(4): 1993–2011.

Lu, W.-S. (2002). A unified approach for the design of 2-D digital filters via semidefinite programming, *IEEE Transactions on Circuits and Systems I: Fundamental Theory and Applications* **49**(6): 814–826.

Lu, W.-S. and Antoniou, A. (1992). *Two-Dimensional Digital Filters, 1st Edition*, CRC Press, New York.

Luenbergerand, D.G. and Ye, Y. (2008). *Linear and Nonlinear Programming*, Kluwer Academic Publishers, Stanford.

Mitra, S.K. and Kaiser, J.K. (1993). *Handbook of Digital Signal Processing*, Wiley-Interscience, New York.

Piekarski, M. and Wirski, R. (2005). On the transfer matrix synthesis of two-dimensional orthogonal systems, *Proceedings of the 2005 European Conference on Circuit Theory and Design, Cork, Ireland*, Vol. 3, pp. III/117–III/120.

Puchala, D. (2022). Effective lattice structures for separable two-dimensional orthogonal wavelet transforms, *Bulletin of the Polish Academy of Sciences: Technical Sciences* **70**(3): 1–8.

Rao, C. and Dewilde, P. (1987). On lossless transfer functions and orthogonal realizations, *IEEE Transactions on Circuits and Systems* **34**(6): 677–678.

Roesser, R. (1975). A discrete state-space model for linear image processing, *IEEE Transactions on Automatic Control* **20**(1): 1–10.

Sienkowski, S. and Krajewski, M. (2021). On the statistical analysis of the harmonic signal autocorrelation function, *International Journal of Applied Mathematics and Computer Science* **31**(4): 729–744, DOI: 10.34768/amcs-2021-0050.

Smith III, J.O. (2007). *Introduction to Digital Filters with Audio Applications*, W3K Publishing, Stanford.

Soman, A. and Vaidyanathan, P. (1995). A complete factorization of paraunitary matrices with pairwise mirror-image symmetry in the frequency domain, *IEEE Transactions on Signal Processing* **43**(4): 1002–1004.

Stancic, S., Rajovic, V. and Slijepcevic, I. (2018). Performance of FPGA implementation of the orthogonal two-channel filter bank for perfect reconstruction, *26th Telecommunications Forum, TELFOR 2018, Belgrade, Serbia*, pp. 1–4.

Vaidyanathan, P. and Mitra, S. (2019). Robust digital filter structures: A direct approach, *IEEE Circuits and Systems Magazine* **19**(1): 14–32.

Valkova-Jarvis, Z., Stoynov, V. and Mihaylova, D. (2019). Designing efficient bilinear bicomplex orthogonal digital filters, *IEEE Conference on Microwave Theory and Techniques in Wireless Communications, MTTW 2019, Riga, Latvia*, pp. 5–8.

Wang, J., Chen, Y., Chakraborty, R. and Yu, S. (2020). Orthogonal convolutional neural networks, *IEEE/CVF Conference on Computer Vision and Pattern Recognition, CVPR 2020, Seattle, USA*, pp. 11502–11512.

Wawryn, K. and Wirski, R. (2009). Synthesis of 2-D lossless FIR filter transfer function matrix, *2009 7th International Conference on Information, Communications and Signal Processing, ICICS 2009, Macau, China*, pp. 1–5.

Wawryn, K., Wirski, R. and Strzeszewski, B. (2010). Implementation of finite impulse response systems using rotation structures, *International Symposium on Information Theory and Its Applications, ISITA 2010, Taichung, Taiwan*, pp. 606–610.

Wirski, R. (2008). On the realization of 2-D orthogonal state-space systems, *Signal Processing* **88**(11): 2747–2753.

Wirski, R. and Wawryn, K. (2008). Roesser's model realization of 2-D FIR lossless transfer matrices, _2008 International Symposium on Information Theory and Its Applications, Auckland, New Zealand_, pp. 1–6.

Wnuk, M. (2008). Remarks on hardware implementation of image processing algorithms, _International Journal of Applied Mathematics and Computer Science_ **18**(1): 105–110, DOI: 10.2478/v10006-008-0010-2.

Yang, Y., Zhu, W.-P. and Yan, J. (2017). Minimax design of orthogonal filter banks with sparse coefficients, _30th IEEE Canadian Conference on Electrical and Computer Engineering, CCECE 2017, Windsor, Canada_, pp. 1–4.

Krzysztof Wawryn received his MS, PhD and DSc degrees in 1976, 1985 and 1992, respectively, all in electronics and from the Gdańsk University of Technology, Poland. In 1998 he was awarded the professorial title by the President of the Republic of Poland. He joined the Koszalin University of Technology, Poland, in 1980, where he then carried out research on the design of analog ICs, switched current circuits and analog neural networks. He is the author of three books and more than 190 articles. His current interests are 2D and 3D loss-less signal processing and hardware implementation of neural networks.

Paweł Poczekajło holds BS and MS degrees in electronics, and a PhD degree in computer science (2019) from the Koszalin University of Technology. He joined the Faculty of Electronics and Computer Science of that university in 2012, where he then carried out research on digital signal processing and orthogonal systems. Since 2019, he has been an assistant professor. His research interests include also programmable microcontrollers and FPGA chips, automation controllers and systems, computer networks, network services and cloud computing.

Appendix

The Scilab code for a 5×5 example filter is as follows (some assignments and argument lists have been simplified due to the large number of elements):

```
//input H 5x5 matrix - example
H=[ 1  1  1  1  1
    1  1  1  1  1
    1  1  1  1  1
    1  1  1  1  1
    1  1  1  1  1]./25

CH=zeros(41,1)
CG1=zeros(41,1)
CG2=zeros(41,1)
Y=[zeros(40,1);1]
JG1=zeros(41,25)
JG2=zeros(41,25)
x=[(CH)' zeros(9,1)']
e=1

for i=1:41 then
    //function to calculate values of
    //i-element of the CH() vector
    CH(i)=get_value_for_ch(i,H)
end
```

```
while e>=10^-7 do
    g144=x(1)
    g143=x(2)
    ...
    g101=x(24)
    g100=x(25)

    g244=x(26)
    g243=x(27)
    ...
    g201=x(49)
    g200=x(50)

    for i=1:41 then
        //function to calculate a
        //i-element of the CG1() vector
        CG1(i)=get_value_for_ch(i,g100,
         ...,g144)
        //function to calculate a
        //i-element of the CG2() vector
        CG2(i)=get_value_for_ch(i,g200,
         ...,g244)
    end

    //function to calculate elements
    //of the JG1() matrix
    JG1=set_value_jg1(g100,...,g144)
    //function to calculate elements
    //of the JG2() matrix
    JG2=set_value_jg1(g200,...,g244)

    F=CH+CG1+CG2-Y
    J=[JG1 JG2]
    delta=(pinv(J)*F)'
    x=(x-delta)
    e=abs(mean(delta))
end

G1= [g100 g110 g120 g130 g140
     g101 g111 g121 g131 g141
     g102 g112 g122 g132 g142
     g103 g113 g123 g133 g143
     g104 g114 g124 g134 g144]

G2= [g200 g210 g220 g230 g240
     g201 g211 g221 g231 g241
     g202 g212 g222 g232 g242
     g203 g213 g223 g233 g243
     g204 g214 g224 g234 g244]
```